Microchimica Acta (2024) 191:23
https://doi.org/10.1007/s00604-023-06107-0

ORIGINAL PAPER

Electrochemiluminescent bioassay based on Ru@Zr-BTC-MOFs nanoparticles for determination of let-7a miRNA using the hybridization chain reaction

Fei Meng[1] · Yisi Wang[1] · Xinxin Lv[1] · Fang Feng[1] · Gongjun Yang[1]

Received: 10 July 2023 / Accepted: 19 November 2023 / Published online: 13 December 2023

Abstract

Carboxyl-rich tris(4,4′-dicarboxylic acid-2,2′-bipyridyl) ruthenium(II) ($[Ru(dcbpy)_3]^{2+}$) and 1,3,5-phenyl tricarboxylic acid (H_3BTC) were used as the organic ligand to synthesize the metal−organic frameworks by a simple one-pot hydrothermal method with $ZrCl_4$ as metal ion source. Subsequently, the excellent electrochemiluminescence (ECL) luminophore (denoted as Ru@Zr-BTC-MOFs) was obtained. The Ru@Zr-BTC-MOFs displayed outstanding ECL properties, and a sensitive ECL bioassay based on Ru@Zr-BTC-MOFs was designed for the detection of let-7a microRNA (miRNA) using hybrid chain reaction (HCR). Under the optimal experimental conditions, the proposed bioassay exhibited a good linear relationship in the range from 50.0 fM to 5.00×10^2 pM with a detection limit of 3.71 fM. Besides, the proposed sensor exhibited satisfactory performance in real samples. The recovery was 91 ~ 108%, and the relative standard deviation was less than 5.6%. It might have potential clinical applications for detecting miRNA in biomedical research and clinical diagnosis.

Keywords Electrochemiluminescence sensor · Aptamer · Hybrid chain reaction · Let-7a · Metal−organic frameworks

Introduction

Cancer is still one of the most widespread causes of death in human beings due to various difficulties in early diagnosis and late clinical treatment of cancer [1]. In recent years, studies have reported that the expression of let-7a (a sort of microRNA) might be related to many cancers. miRNA is a kind of non-coding small RNA composed of 19-23 nucleotides [2]. Its abnormal expression level is closely related to cancer [3], cardiovascular disease [4], and so on. However, due to the short size and highly similar sequence of miRNAs, there are still considerable challenges to accurately determine miRNA [5].

At present, many classical technologies, such as microarrays [6], real-time PCR [7] and northern blotting [8], have been applied in miRNA detection. But these technologies had their own unavoidable shortcomings [9, 10]. In order to avoid these shortcomings, many new methods of capillary electrophoresis [11], electrochemiluminescence [12] and fluorescence [13] in nucleic acid detection have gradually attracted the attention of researchers. As to electrochemical sensor, on the one hand, the electrochemical technology does not require tedious pretreatment processes and complicated operation procedure, and its instruments are relatively inexpensive and portable. On the other hand, due to the development of electrode modification and surface fixation technology, molecular recognition and sensing can be achieved on the electrode surface without excessive intervention. The electrochemiluminescence method showed great application prospects because of its advantages, such as high specificity of biological receptors, low background signal, low detection limit and easy operation [14, 15].

Metal-organic frameworks (MOFs) [16, 17], as a porous variant of coordination polymer with the advantages of large surface area, remarkable porosity and easy modification and

Fei Meng and Yisi Wang contributed equally to this work.

✉ Fang Feng
fengfang1@126.com

✉ Gongjun Yang
gjyang@cpu.edu.cn; yanggongjun888@163.com

[1] Key Laboratory of Drug Quality Control and Pharmacovigilance (China Pharmaceutical University), Ministry of Education, School of Pharmacy, China Pharmaceutical University, Nanjing 211198, People's Republic of China

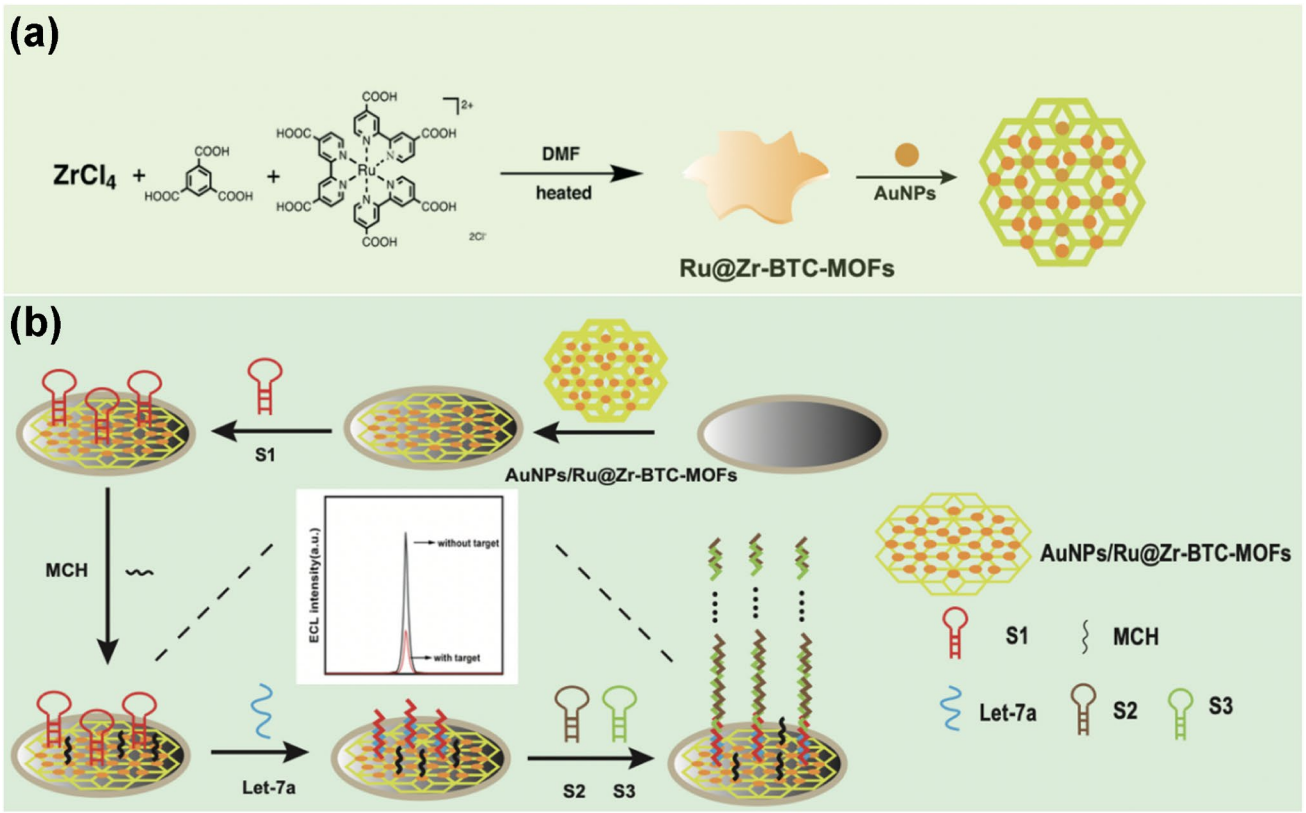

Scheme 1 The schematic diagram of the preparation of Ru@Zr-BTC-MOFs (**a**) and ECL sensor for detecting let -7a (**b**)

functionalization, have attracted great interest. Owing to these excellent properties, MOFs have been widely applied in gas storage/separation [18–20], drug delivery [21], heterogeneous catalysis [22] and biosensing [23]. Recently, MOFs have been employed as carrier materials to increase the immobilization amount of ECL luminophores [24, 25].

$[Ru(dcbpy)_3]Cl_2$, a carboxylated ruthenium structure of tripyridine ruthenium chloride hexahydrate, could not only be luminophores with the same high electrochemical luminescence signal as $[Ru(bpy)_3]Cl_2$, but also be the ligand through its carboxyl coordinating with metal ions. The sheet-like nanomaterial structure can greatly shorten the diffusion paths of ions, electrons, co-reactants and so on, which improves the utilization ratio of luminophores. On the other hand, $[Ru(dcbpy)_3]Cl_2$ as a bridging ligand could connect two Zr_{12} clusters of 2D Ru@Zr-BTC nanoplate through Zr-O bonds, which was beneficial to enhance the stability of the ECL signal. As mentioned above, Ru@Zr-BTC nanoplate exhibited superior ECL performance in high ECL response and excellent stability, making it a promising candidate for constructing highly sensitive ECL biosensors.

In this study, a new metal-organic framework material of Ru@Zr-BTC-MOFs, as an indicator of ECL signal, was synthesized. And the ultrasensitive electrochemiluminescence bioassay based on Ru@Zr-BTC-MOFs nanoparticles was fabricated to detecting Let-7a using the hybridization chain reaction [26], which was a common signal amplification strategy without enzyme participation (Scheme 1). The solution of Ru@Zr-BTC-MOFs and AuNPs were mixed and dropped on the surface of bare glassy carbon electrode (GCE) to form AuNPs/Ru@Zr-BTC-MOFs film with high ECL response. Then, sulfhydryl-modified aptamer S1 was fixed on the surface of the electrode through Au-S bond. In the presence of the target let-7a, the hairpin structure of S1 was opened and hybridized with its complementary single-chain DNA S2 and S3 to complete the hybrid chain reaction. Thus, the proposed aptamer ECL sensor would realize to significantly improve the sensitivity for determining let-7a in real samples with satisfactory results. It might provide a potential approach for the diagnosis of cancers.

Experimental section

Reagents and apparatus

The reagents and apparatus used for the study are listed in the Supplementary Information (S1 Reagents and apparatus).

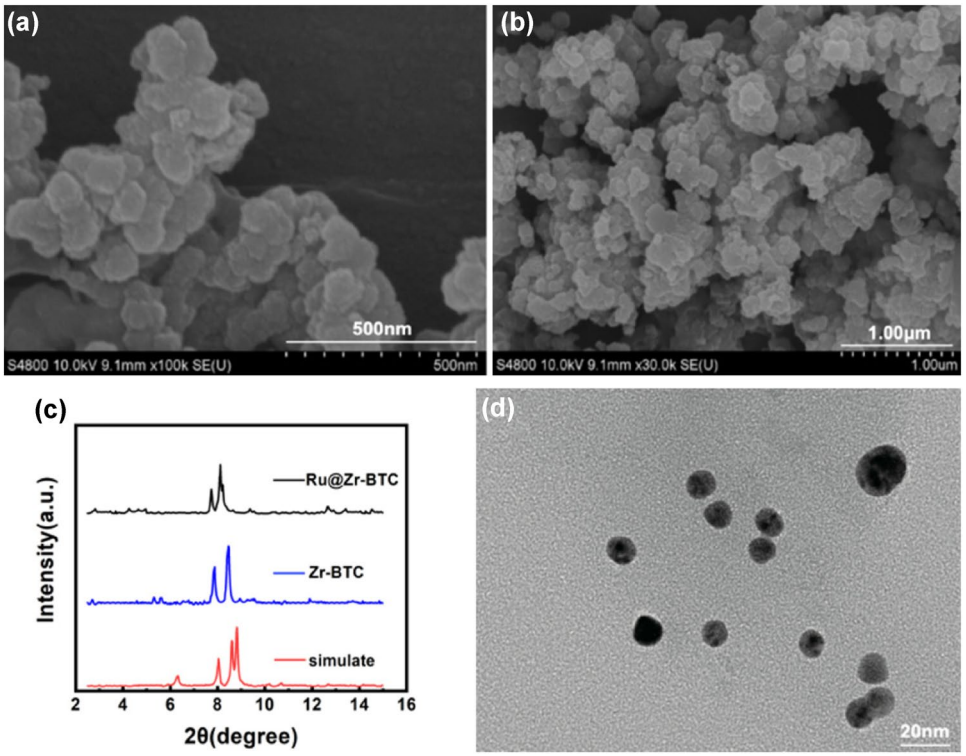

Fig. 1 SEM images of the prepared Ru@Zr-BTC-MOFs (**a** and **b**). The PXRD patterns of Ru@Zr-BTC-MOFs and Zr-BTC-MOFs (**c**). TEM image of AuNPs (**d**)

Synthesis of gold nanoparticles (AuNPs)

AuNPs were synthesized according to a previous report with some modification [27]. The detailed procedures are listed in the Supplementary Information (S2 Synthesis of gold nanoparticles (AuNPs)).

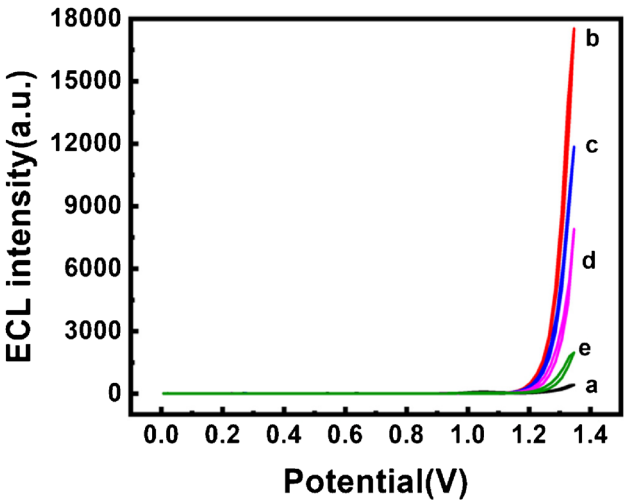

Fig. 2 The ECL signals of each step in the process of preparing the bioassay. a: bare GCE, b: AuNPs/Ru@Zr-BTC-MOFs/GCE, c: S1/AuNPs/Ru@Zr-BTC-MOFs/GCE,d: MCH/S1/AuNPs/Ru@Zr-BTC-MOFs/GCE, e: Let-7a/S2/S3/MCH/S1/AuNPs/Ru@Zr-BTC-MOFs/GCE. The PMT was set at 800 V

Synthesis of Ru@Zr-BTC-MOFs nanomaterials

Ru@Zr-BTC was prepared referring to previous report with some modifications [28, 29]. Firstly, 4.2 mg $ZrCl_4$, 3.9 mg H_3BTC and 1.3 mg $[Ru(dcbpy)_3]Cl_2$ were dissolved in 4 mL DMF. Subsequently, 1 mL doubly-distilled water was added into above solution and sonicated for 10 min. Then, the mixture solution was transferred into a 7 mL vial and heated at 120°C for 48 h. After cooling to room temperature, the resultant orange suspension was collected by centrifugation at 8000 rpm for 5 min, and washed with DMF and doubly-distilled water, respectively. Finally, the product was dispersed into 1 mL doubly-distilled water and stored at 4°C in the dark place for further use.

Analysis of agarose gel electrophoresis

The detailed process listed in the Supplementary Information (S3 Analysis of Agarose Gel Electrophoresis).

Fabrication of the ECL biosensor

The fabrication of the proposed biosensor was shown in Scheme 1b. Firstly, the bare GCE was polished to a mirror-like surface by sequentially using 0.3 and 0.05 μm alumina slurry, followed by sonication in ethanol and doubly-distilled

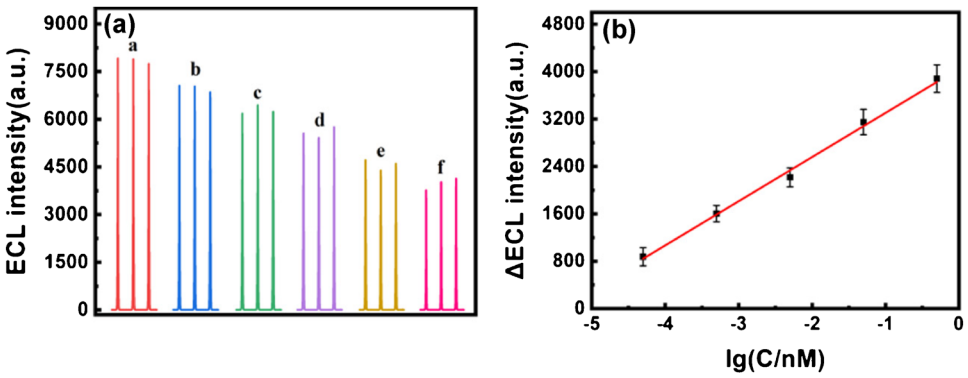

Fig. 3 (**a**) ECL signals of the biosensor at the different let-7a concentrations. (a~f: 0.00, 50.0 fM, 5.00 × 10^2 fM, 5.00 pM, 50.0 pM, 5.00 × 10^2 pM) (**b**) Linear relationship between ECL intensity and logarithm of let-7a concentration. PMT: 800 V, S2 and S3 concentration: 2.5μM

water to remove any residues, respectively. And then it allowed to dry at room temperature. First, the mixed solution of 6.0 μL AuNPs and 5.0 μL Ru@Zr-BTC-MOFs was placed on the surface of GCE and dried completely (denoted as AuNPs/Ru@Zr-BTC-MOFs/GCE). Then 5.0 μL S1 (2.5 μM) was added on the surface of AuNPs/Ru@Zr-BTC-MOFs/GCE to incubate for 12 h at room temperature (denoted as S1/AuNPs/Ru@Zr-BTC-MOFs/GCE). When the electrode was further immersed in 1 mM MCH for 60 minutes to block the unresponsive active site (denoted as MCH/S1/AuNPs/Ru@Zr-BTC-MOFs/GCE), the mixture solution of 3.0 μL Let-7a, 3.0 μL S2 (2.5 μM) and 3.0 μL S3 (2.5 μM) was dropped on the surface of MCH/S1/AuNPs/Ru@Zr-BTC-MOFs/GCE to incubate for 150 minutes at room temperature. After each step of the construction of the biosensor, the electrode surface was washed with doubly-distilled water to remove the unbound substances.

Preparation of samples

In this study, serum samples were obtained from several patients with a history of malignant breast cancer and normal people from Jiangsu Cancer Hospital. Three hundred microliter serum sample was diluted with 1.0 mL 0.1 M phosphate buffer solution (PBS, pH 7.4), and then centrifuge at 10000 rpm for 5 min. The supernatant was collected and stored at 4°C for further use. As to recovery test, the known concentration of let-7a was added to the real sample, and the pretreatment procedure was the same as the previous sample processing.

Results and discussion

Characterization of Ru@Zr-BTC-MOFs nanoparticles

The morphologies of the prepared Ru@Zr-BTCs-MOFs were characterized by SEM. As shown in Fig. 1a and b, the Ru@Zr-BTCs-MOFs presented irregular nanoplate like sheet oatmeal. Moreover, the powder X-ray diffraction (PXRD) patterns of Ru@Zr-BTC-MOFs and Zr-BTC-MOFs showed several peaks in 2θ, ranged between 3.7 and 15° which matched with the simulated PXRD pattern well (Fig. 1c), suggesting that Ru@Zr-BTC was iso-structural with the parent framework of Zr-BTC-MOFs [30]. These results demonstrated that the Ru@Zr-BTC-MOFs was successfully synthesized. According to the transmission electron microscopy (TEM) image (Fig. 1d), the size of AuNPs was about 16 nm with a spherical morphology.

Characterization of the HCR process

To validate the feasibility of HCR, gel electrophoresis assay was performed.

The results were in the Supplementary Information (S4. Characterization of the HCR Process), which indicated that DNA nanostructures based on HCR were successfully constructed and the HCR amplification procedure was feasible.

Table 1 Comparison of sensitivities of this work with some available methods

Methods	Detection range (pM)	Detection limit (pM)	References
Fluorescence	5.0 ~ 5.0×10^2	3.8	[31]
Microarrays	1.0×10^{-2} ~ 1.0×10^2	1×10^{-2}	[32]
LCR	2.0 ~ 2.0×10^3	0.7	[33]
ECL	1.0×10^{-2} ~ 1.0	3×10^{-3}	[34]
Lateral flow assay	1.0×10^2 ~ 2.0×10^3	1.14×10^2	[35]
EIS	1.0×10^{-2} ~ 1.0×10^3	4.2×10^{-3}	[35]
ECL	5.0×10^{-2} ~ 5.0×10^2	3.71×10^{-3}	This work

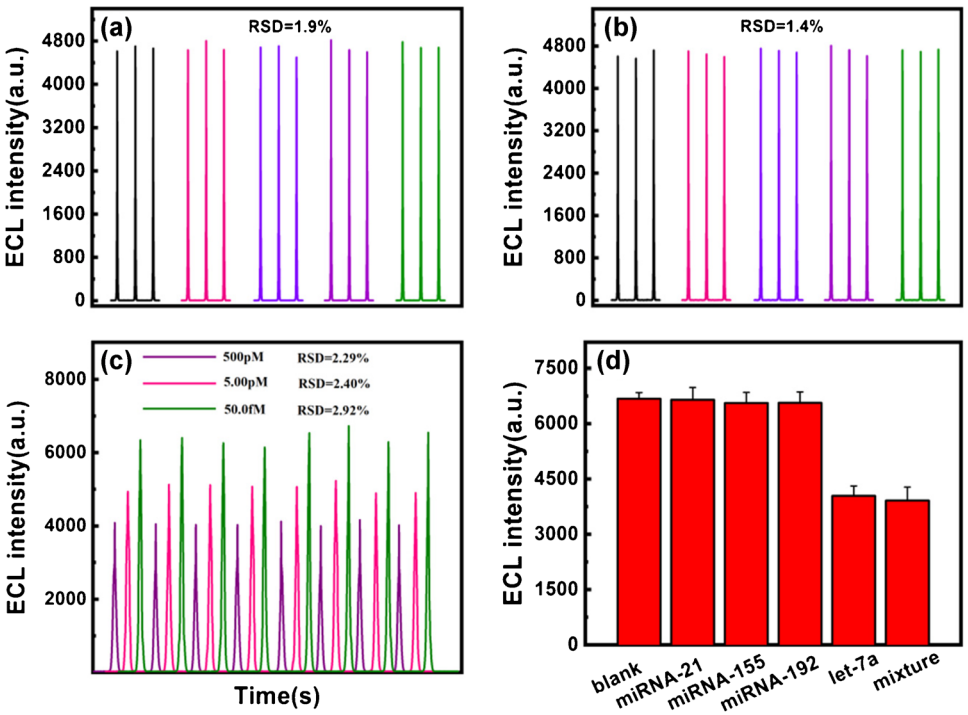

Fig. 4 Reproducibility (**a**), repeatability (**b**), stability (**c**) and seledctivity (**d**) of the proposed biosensor

Characterization of the proposed bioassay

The successful manufacture of the aptamer sensor was verified by electrochemiluminescence (ECL). As shown in Fig. 2, there was almost no ECL response at bare GCE (curve a). After dropping AuNPs/Ru@Zr-BTC-MOFs on the surface of GCE, the ECL signal increased significantly (curve b). However, when the AuNPs/Ru@Zr-BTC-MOFs/GCE was incubated with S1 and MCH, respectively, the ECL response decreased significantly (curve c and curve d) because S1 and MCH blocked the electron transfer. When S2, S3 and target let-7a were added to the MCH/S1/AuNPs/Ru@Zr-BTC-MOFs/GCE, the ECL strength was further reduced (curve e). It showed that the participation of target let-7a caused the hairpin structure of S1 to open and then conducted hybrid chain reaction with S2 and S3. Electrochemical impedance spectroscopy (EIS) and cyclic voltammetry (CV) was also used to manifest the manufacturing process of the adapter sensor in 0.1 M PBS (pH 7.4) containing 5.0 mM $[Fe(CN)_6]^{3-/4-}$. These results were given in Supplementary Information (S4 Characterization of the Proposed Bioassay), which manifested the successful preparation of the ECL bioassay.

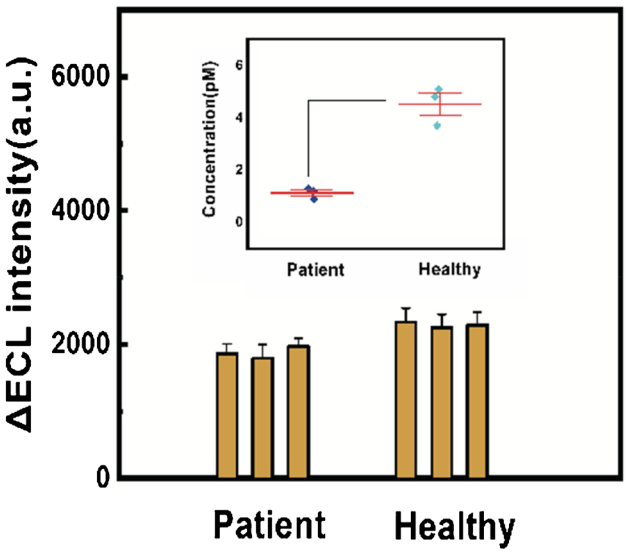

Fig. 5 The ΔECL intensity of the proposed biosensor for the detection of let-7a expressed in three diluted serum samples from patients diagnosed with breast cancer and three serum samples from healthy persons. The inset was the quantization diagram in diluted sample tests. (let-7a addition: 0 pM)

Optimum of experimental conditions

In order to improve the detection performance of ECL aptamer sensor, some factors, such as the volume of Ru@Zr-BTC-MOFs and AuNPs, concentration of aptamer S1 and time of HCR reaction, were optimized. The detailed experimental results were listed in Supplementary Information (S5 Optimum of Experimental Conditions). 5.0 μL of Ru@Zr-BTC and 6.0 μL of AuNPs on the GCE, 2.5 μM S1 concentration, 150 min of hybridization time between target and S1, S2 were chosen in the subsequent experiments.

Table 2 Detection of let-7a in diluted serum samples by the proposed method

Sample	Detection Result of sample (pM)	PCR detection result (pM)	Added (pM)	Found (pM)	Recovery (%)	RSD(%)(n=3)
serum[a]	1.21	1.12	5.0	5.82	92%	3.4%
			50.0	51.7	101%	2.9%
serum[b]	0.93	0.78	5.0	5.50	91%	5.6%
			50.0	52.3	103%	3.8%
serum[c]	3.71	3.52	5.0	9.13	108%	5.4%
			50.0	52.8	98%	3.5%
serum[d]	4.84	4.69	5.0	10.1	105%	4.2%
			50.0	55.2	101%	4.7%

*a and b: patient

**c and d: healthy individuals

Analytical performance of the bioassay

Under the optimized experimental conditions, the ECL curve of the biosensor in different let-7a concentrations was recorded (Fig. 3a). It can be seen that ECL intensity decreased with the increase of let-7a concentration. Based on the data analysis in Fig. 3b, ΔECL (ΔECL was the difference of the ECL intensity values between detected in the reaction solution without let-7a participating and detected under the different concentrations let-7a participates in HCR solution, that is, $\Delta ECL = ECL_{(MCH/S1/AuNPs/Ru@Zr\text{-}BTC\text{-}MOFs/GCE)} - ECL_{(Let\text{-}7a/S2/S3/MCH/S1/AuNPs/Ru@Zr\text{-}BTC\text{-}MOFs/GCE)}$) and the logarithm of let-7a concentrations showed a good linear relationship in the range of 50.0 fM ~ 5.00×10^2 pM, and the linear equation was $\Delta ECL = 4.050 \times 10^3 + 7.458 \times 10^2 \lg(c / nM)$. The correlation coefficient was 0.9919 and detection limit was 3.71 fM (S /N=3). Compared with other let-7a analysis methods, the proposed method performed a wide linear range and low detection limit (Table 1).

The reproducibility of the biosensor was evaluated by using five different electrodes to detect let-7a with a concentration of 50.0 pM after the same modification, and the relative standard deviation (RSD) of ECL intensity was 1.9% (Fig. 4a). The repeatability of the biosensor was evaluated by using the same electrode modified five times, and the RSD of ECL intensity was 1.4% (Fig. 4b). In addition, the stability of the proposed ECL biosensor for three let-7a concentrations (50.0 fM, 5.00 pM, 5.00×10^2 pM) showed a relative stable curve with successive scanning for 8 cycles, and the RSD of different concentrations were within 2.92% (Fig. 4c). The above experimental results showed the good reproducibility, repeatability and stability of the proposed biosensor.

In order to evaluate the selectivity of the proposed sensor, some different interfering substances, including miRNA-21, miRNA-155 and miRNA-192, were tested. Compared with 1.00×10^2 pM let-7a, the concentration of these interfering substances was set at 0.500 nM. As depicted in Fig. 4d, the interfering substances exhibited little interference with let-7a, which proved that the proposed biosensor performed good selectivity for let-7a detection.

Samples analysis

In order to verify the accuracy of the aptamer sensor, 8 μL of two levels of 5.00 pM and 50.0 pM let-7a were added to 8 μL serum samples respectively using the standard addition method. When let-7a addition was 0, the ΔECL intensity of patient and healthy individuals was shown in Fig. 5, which indicated that let-7a was low expression in breast cancer patients. At the same time, qPCR as a control experiment was used to further verify the accuracy of the proposed electrochemiluminescent bioassay. As shown in Table 2, the results obtained by the proposed method were basically consistent with those of the control experiment. Additionally, the recoveries of the proposed method were between 91% and 108%, and the RSD value was less than 5.6%, indicating that the proposed method performed good accuracy in practical detection and clinical diagnosis.

Conclusion

A novel Ru@Zr-BTC-MOFs with high ECL efficiency were prepared by a simple method and successfully applied for preparing the ECL bioassay to sensitively detect let-7a. It exhibited high sensitivity and a wide linear range. Moreover, the proposed ECL sensor performed good reproducibility, repeatability, stability, selectivity and accuracy for let-7a detection. More importantly, this sensing strategy might pave a general avenue for considerably advancing the field of clinical diagnostics, particularly for early cancer diagnosis and prognosis. This work would widen the application of ultrasensitive analysis with the perspective efficient utilization of nanomaterials and luminescent materials.

Supplementary Information The online version contains supplementary material available at https://doi.org/10.1007/s00604-023-06107-0.

Acknowledgements This work was supported by Jiangsu Provincial Science and Technology Plan Special Fund Key R&D Plan Social Development Project (BE2023841). Thanks for Prof. Chen Yun's research group of Nanjing Medical University to provide the breast cancer samples.

Data availability Data generated or analyzed during this study are included in this published article.

Declarations

Conflict of interest The authors declare no competing interests.

References

1. Bray F, Ferlay J, Soerjomataram I, Siegel RL, Torre LA, Jemal A (2018) Global cancer statistics 2018: GLOBOCAN estimates of incidence and mortality worldwide for 36 cancers in 185 countries. CA Cancer J Clin 68(6):394–424. https://doi.org/10.3322/caac.21492
2. Dong H, Lei J, Ding L, Wen Y, Ju H, Zhang X (2013) MicroRNA: function, detection, and bioanalysis. Chem Rev 113(8):6207–6233. https://doi.org/10.1021/cr300362f
3. Li Y, Liang L, Zhang C-y (2013) Isothermally sensitive detection of serum circulating miRNAs forlung cancer diagnosis. Anal Chem 85(23):11174–11179. https://doi.org/10.1021/ac403462f
4. Liu N, Olson EN (2010) MicroRNA regulatory networks in cardiovascular development. Dev Cell 18(4):510–525. https://doi.org/10.1016/j.devcel.2010.03.010
5. Cissell KA, Deo SK (2009) Trends in microRNA detection. Anal Bioanal Chem 394(4):1109–1116. https://doi.org/10.1007/s00216-009-2744-6
6. Liu CG, Calin GA, Meloon B, Gamliel N, Sevignani C, Ferracin M, Dumitru CD, Shimizu M, Zupo S, Dono M, Alder H, Bullrich F, Negrini M, Croce CM (2004) An oligonucleotide microchip for genome-wide microRNA profiling in human and mouse tissues. Proc Natl Acad Sci USA 101(26):9740–9744. https://doi.org/10.1073/pnas.0403293101
7. Li J, Yao B, Huang H, Wang Z, Sun C, Fan Y, Chang Q, Li S, Wang X, Xi J (2009) Real-Time polymerase chain reaction microRNA detection based on enzymatic stem-loop probes ligation. Anal Chem 81(13):5446–5451. https://doi.org/10.1021/ac900598d
8. Valoczi A, Hornyik C, Varga N, Burgyan J, Kauppinen S, Havelda Z (2004) Sensitive and specific detection of microRNAs by northern blot analysis using LNA-modified oligonucleotide probes. Nucleic Acids Res 32(22):e175. https://doi.org/10.1093/nar/gnh171
9. Li W, Ruan K (2009) MicroRNA detection by microarray. Anal Bioanal Chem 394(4):1117–1124. https://doi.org/10.1007/s00216-008-2570-2
10. Varallyay E, Burgyan J, Havelda Z (2008) MicroRNA detection by northern blotting using locked nucleic acid probes. Nat Protoc 3(2):190–196. https://doi.org/10.1038/nprot.2007.528
11. Ban E, Song EJ (2014) Capillary electrophoresis methods for microRNAs assays: a review. Anal Chim Acta 852:1–7. https://doi.org/10.1016/j.aca.2014.08.034
12. Zhang P, Zhuo Y, Chang Y, Yuan R, Chai Y (2015) Electrochemiluminescent graphene quantum dots as a sensing Platform: a dual Amplification for microRNA assay. Anal Chem 87(20):10385–10391. https://doi.org/10.1021/acs.analchem.5b02495
13. Huang J, Su X, Li Z (2012) Enzyme-free and amplified fluorescence DNA detection using bimolecular beacons. Anal Chem 84(14):5939–5943. https://doi.org/10.1021/ac3004727
14. Irkham, Watanabe T, Fiorani A, Valenti G, Paolucci F, Einaga Y (2016) Co-reactant-on-demand ECL: electrogenerated chemiluminescence by the in situ production of S(2)O(8)(2-) at boron-doped diamond electrodes. J Am Chem Soc 138(48):15636–15641. https://doi.org/10.1021/jacs.6b09020
15. Valenti G, Rampazzo E, Bonacchi S, Petrizza L, Marcaccio M, Montalti M, Prodi L, Paolucci F (2016) Variable doping induces mechanism swapping in electrogenerated chemiluminescence of Ru(bpy)3(2+) core-shell silica nanoparticles. J Am Chem Soc 138(49):15935–15942. https://doi.org/10.1021/jacs.6b08239
16. He J, Zhang G, Xiao D, Chen H, Yan S, Wang X, Yang J, Wang E (2012) Helicity controlled by the chirality of amino acid: two novel enantiopure chiral 3D architectures containing fivefold interwoven helices. CrystEngComm 14:3609–3614. https://doi.org/10.1039/c2ce25038a
17. Chen H, Xiao D, Fan L, He J, Yan S, Zhang G, Sun D, Ye Z, Yuan R, Wang E (2011) Unusual self-threading and interdigitated architectures self-assembled from long flexible ligands and d10 metal salts. CrystEngComm 13:7098–7107. https://doi.org/10.1039/c1ce05573a
18. Vitillo JG, Regli L, Chavan S, Ricchiardi G, Spoto G, Dietzel PDC, Bordiga S, Zecchina A (2008) Role of exposed metal sites in hydrogen storage in MOFs. J Am Chem Soc 130(26):8386–8396. https://doi.org/10.1021/ja8007159
19. Jun JW, Tong M, Jung BK, Hasan Z, Zhong C, Jhung SH (2015) Effect of central metal ions of analogous metal-organic frameworks on adsorption of organoarsenic compounds from water: plausible mechanism of adsorption and water purification. Chemistry 21(1):347–354. https://doi.org/10.1002/chem.201404658
20. Centrone A, Santiso EE, Hatton TA (2011) Separation of chemical reaction intermediates by metal-organic frameworks. Small 7(16):2356–2364. https://doi.org/10.1002/smll.201100098
21. Zhuang J, Kuo C-H, Chou L-Y, Liu D-Y, Weerapana E, Tsung C-K (2014) Optimized metal–organic-framework nanospheres for drug delivery: evaluation of small-molecule encapsulation. ACS Nano 8(3):2812–2819. https://doi.org/10.1021/nn406590q
22. Cui C, Liu Y, Xu H, Li S, Zhang W, Cui P, Huo F (2014) Self-assembled metal-organic frameworks crystals for chemical vapor sensing. Small 10(18):3672–3676. https://doi.org/10.1002/smll.201302983
23. Zhou Y, Zhuo Y, Liao N, Chai Y, Yuan R (2014) Ultrasensitive immunoassay based on a pseudobienzyme amplifying system of choline oxidase and luminol-reduced Pt@Au hybrid nanoflowers. Chem Commun (Camb) 50(93):14627–14630. https://doi.org/10.1039/c4cc05269b
24. Hu GB, Xiong CY, Liang WB, Zeng XS, Xu HL, Yang Y, Yao LY, Yuan R, Xiao DR (2018) Highly stable mesoporous luminescence-functionalized MOF with excellent electrochemiluminescence property for ultrasensitive immunosensor construction. ACS Appl Mater Interfaces 10(18):15913–15919. https://doi.org/10.1021/acsami.8b05038
25. Xiong C, Liang W, Zheng Y, Zhuo Y, Chai Y, Yuan R (2017) Ultrasensitive assay for telomerase activity via self-enhanced electrochemiluminescent ruthenium complex doped metal-organic frameworks with high emission efficiency. Anal Chem 89(5):3222–3227. https://doi.org/10.1021/acs.analchem.7b00259

26. Dirks RM, Pierce NA (2004) Triggered amplification by hybridization chain reaction. Proc Natl Acad Sci USA 101(43):15275–15278. https://doi.org/10.1073/pnas.0407024101
27. Pang L, Li J, Jiang J, Shen G, Yu R (2006) DNA point mutation detection based on DNA ligase reaction and nano-Au amplification: a piezoelectric approach. Anal Biochem 358(1):99–103. https://doi.org/10.1016/j.ab.2006.06.038
28. Wang C, Xie Z, deKrafft KE, Lin W (2011) Doping metal-organic frameworks for water oxidation, carbon dioxide reduction, and organic photocatalysis. J Am Chem Soc 133(34):13445–13454. https://doi.org/10.1021/ja203564w
29. Dai R, Peng F, Ji P, Lu K, Wang C, Sun J, Lin W (2017) Electron crystallography reveals atomic structures of metal-organic nanoplates with M12(μ3-O)8(μ3-OH)8(μ2-OH)6 (M = Zr, Hf) secondary building units. Inorg Chem 56(14):8128–8134. https://doi.org/10.1021/acs.inorgchem.7b00845
30. Abuzalat O, Homayoonnia S, Wong D, Tantawy HR, Kim S (2021) Facile and rapid synthesis of functionalized Zr-BTC for the optical detection of the blistering agent simulant 2-chloroethyl ethyl sulfide (CEES). Dalton Trans 50(9):3261–3268. https://doi.org/10.1039/d0dt04382f
31. Li Y, Zhang J, Zhao J, Zhao L, Cheng Y, Li Z (2016) A simple molecular beacon with duplex-specific nuclease amplification for detection of microRNA. Analyst 141(3):1071–1076. https://doi.org/10.1039/c5an02312b
32. Li Z, Zhao B, Wang D, Wen Y, Liu G, Dong H, Song S, Fan C (2014) DNA nanostructure-based universal microarray platform for high-efficiency multiplex bioanalysis in biofluids. ACS Appl Mater Interfaces 6(20):17944–17953. https://doi.org/10.1021/am5047735
33. Yan J, Li Z, Liu C, Cheng Y (2010) Simple and sensitive detection of microRNAs with ligase chain reaction. Chem Commun (Camb) 46(14):2432–2434. https://doi.org/10.1039/b923521c
34. Chang Z, Wang Y, Zheng X (2016) Electrochemiluminescence (ECL) detection of MicroRNAs using polyethylenimine (PEI)/SiO 2 nanoparticles as the indicator. J Electroanal Chem 780:201–208. https://doi.org/10.1016/j.jelechem.2016.09.015
35. Song Z, Zhang QY, Li JJ, Su JL, Liu YH, Yang GJ, Wang HS (2023) Visual and electrochemical detection of let-7a: A tumor suppressor and biomarker. J Med Chem 66(11):7605–7614. https://doi.org/10.1021/acs.jmedchem.3c00499